

# Nuclear data evaluation of $^{206}\text{Pb}$ for proton- and neutron-induced reaction in energy region from 20 to 200 MeV

Tsuyoshi Kajimoto<sup>1</sup>, Nobuhiro Shigyo<sup>1</sup>, Kenji Ishibashi<sup>1</sup>, Satoshi Kunieda<sup>2</sup>,  
and Tokio Fukahori<sup>2</sup>

<sup>1</sup>*Kyushu University, 744 Nishi-ku, Motoooka, Fukuoka 819-0395 Japan*

<sup>2</sup>*Japan Atomic Energy Agency, Tokai, Naka, Ibaraki 319-1195, Japan*

Nuclear data evaluation was carried out for  $^{206}\text{Pb}$  for proton and neutron incidence in the energy range from 20 to 200 MeV by using the ECIS-96 and the GNASH code. Evaluated cross sections were compared with measurement data and the LA150 evaluations.

## 1 Introduction

The evaluated nuclear data in the intermediate energy range for various nuclei are required such technologies as spallation neutron sources, accelerator shielding design, radiation therapy, and space developments. The program for completion of the JENDL High Energy File (JENDL-HE)<sup>1</sup> is now ongoing under the Japanese Nuclear Data Committee to meet these needs. The 2007 version of JENDL-HE will be published this year.

In the shielding design of high energy accelerators, lead is one of the important shield element. Evaluating nuclear data for lead is necessary to the recent and the future nuclear technologies. In this work, the evaluation of neutron and proton induced nuclear data for  $^{206}\text{Pb}$  was performed using the GNASH code system. The evaluations for neutron incidence were started at 20 MeV that was the upper limit of existing data files for fission and fusion reactors.

The optical model analysis was carried out as the initial approach. The ECIS-96 code<sup>2</sup> was adopted for the optical model calculation. It was also applied to obtain transmission coefficients of induced- and outgoing-particles which were required for the statistical model calculations, and to evaluate elastic- and inelastic- scattering, total and total-reaction cross sections. The GNASH code<sup>3</sup> was used in order to calculate light particle spectra and isotope-production cross sections. The code employed the Hauser-Feshbach model for statistical decay process, and the exciton model for pre-equilibrium processes.

We made evaluations for such values of total, total-reaction, angular-differential elastic-scattering, energy-differential particle-production, and double-differential particle-production cross sections. The validities of calculated excitation functions for isotope-production cross sections were also investigated. Present results were compared with the LA150<sup>4</sup> evaluations.

## 2 Optical model calculation

The optical model is one of the most efficient method to calculate angular-differential elastic-scattering, total and total reaction cross sections. In the model calculation, the optical model potential (OMP) parameters were essential to be optimized. They are also

important values to provide transmission coefficient required in the statical model calculation. Therefore, the optical potential was searched for so as to obtain good descriptions of measured data. In this work, we assumed the OMP could be described with following functional forms.

$$V_R = \left( V_R^0 + V_R^1 E^\dagger + V_R^2 E^{\dagger 2} + V_R^{DISP} e^{-\lambda_R E^\dagger} \right) \left[ 1 + \frac{1}{V_R^0 + V_R^{DISP}} (-1)^{Z'+1} C_{viso} \frac{N-Z}{A} \right] + C_{coul} \frac{ZZ'}{A^{1/3}} \rho_{coul} \left( E^\dagger \right), \quad (1)$$

$$W_V = W_V^{DISP} \frac{E^{\dagger 2}}{E^{\dagger 2} + WID_V^2}, \quad (2)$$

$$W_D = \left[ W_D^{DISP} + (-1)^{Z'+1} C_{wiso} \frac{N-Z}{A} \right] e^{-\lambda_D E^\dagger} \frac{E^{\dagger 2}}{E^{\dagger 2} + WID_D^2}, \quad (3)$$

$$V_{SO} = V_{SO}^0 e^{-\lambda_{SO} E^\dagger}, \quad (4)$$

$$W_{SO} = W_{SO}^{DISP} \frac{E^{\dagger 2}}{E^{\dagger 2} + WID_{SO}^2}. \quad (5)$$

The functions were proposed by Soukhovitskii et al.<sup>5)</sup> The symbols  $V_R$ ,  $W_V$ ,  $W_D$ ,  $V_{SO}$  and  $W_{SO}$  correspond to real volume, imaginary volume, imaginary surface, real and imaginary spin-orbit terms of potential depths in MeV, respectively. The spin-orbit parameters were taken from those of Koning and Delaroche.<sup>6)</sup> The parameters  $A$ ,  $Z$ ,  $N$  and  $Z'$  are the numbers of nucleon, proton, neutron in target nucleus and charge-number of projectile particle, respectively. The  $E^\dagger$  expresses the relative projectile-energy to the Fermi energy  $E_f$ . The  $\rho_{coul}$  stands for the Coulomb term which is written as follows.

$$\rho_{coul} = \left( \lambda_R V_R^{DISP} e^{-\lambda_R E^\dagger} - V_R^1 - 2V_R^2 E^\dagger \right) \left[ 1 + \frac{1}{V_R^0 + V_R^{DISP}} (-1)^{Z'+1} C_{viso} \frac{N-Z}{A} \right]. \quad (6)$$

The Woods-Saxon form  $f_{R,D,V,SO}$  was utilized to described geometries of the optical potential. The optical potential is described as,

$$V(r) = -V_R f_R(r) + i \left[ 4W_D a_D \frac{d}{dr} f_D(r) - W_V f_V(r) \right] + \left( \frac{\hbar}{m\pi c} \right)^2 (V_{SO} + iW_{SO}) \frac{1}{r} \frac{d}{dr} f_{SO}(r) \mathbf{L} \cdot \boldsymbol{\sigma} + V_{Coul}(r). \quad (7)$$

The symbols  $\mathbf{L}$  and  $\boldsymbol{\sigma}$  stand for the orbital angular-momentum for the relative motion and the Pauli matrices of projectile. The  $V_{Coul}(r)$  indicates the Coulomb potential.

At first, the OMP parameters were searched for the neutron-incidence interactions. The initial OMP parameters were taken from the local parameter set proposed by Kunieda et al.<sup>7)</sup> Parameters  $V_R^{0-2,DISP}$ ,  $\lambda_{R,D}$ ,  $W_D^{DISP}$ , and  $WID_{D,V}$  were adjusted so as to obtain accurate descriptions of measured total and elastic scattering differential cross sections. The determined OMP parameters are listed in **Table 1**. The evaluated total and angular-differential elastic-scattering cross sections are shown together with experimental data in **Figs. 1** and **2**, respectively. The characteristic of proton and neutron is analogous except for the Coulomb effects. Therefore, the OMP parameters for proton were determined by modifying those for neutron. The determined OMP parameters for proton are also listed in Table 1. Figure 2 gives evaluated proton-induced angular-differential elastic-scattering cross sections together with measured data. Good agreements were seen between calculated and experiment data.

Table 1: OMP parameters used in evaluation of  $^{206}\text{Pb}$ .

	neutron	proton
$V_R^0$	-35.3	-39.5
$V_R^1$	0.02	0.03
$V_R^2$	0.000145	0.000125
$V_R^{DISP}$	93.28	99.18
$\lambda_R$	0.0045	0.00445
$W_D^{DISP}$	16.5	15.0
$WID_D$	16.0	9.0
$\lambda_D$	0.0185	0.0155
$W_V^{DISP}$	18.0	17.0
$WID_V$	110.0	105.0
$a$	0.671	0.671
$E_f$	-8.09	-7.25

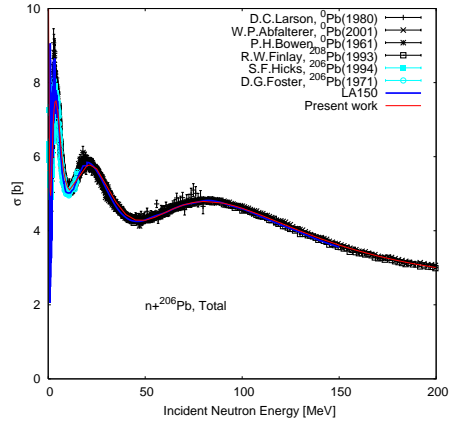


Fig. 1: Present evaluation and measured data<sup>9)</sup> for neutron-induced total cross sections on  $^{206}\text{Pb}$ .

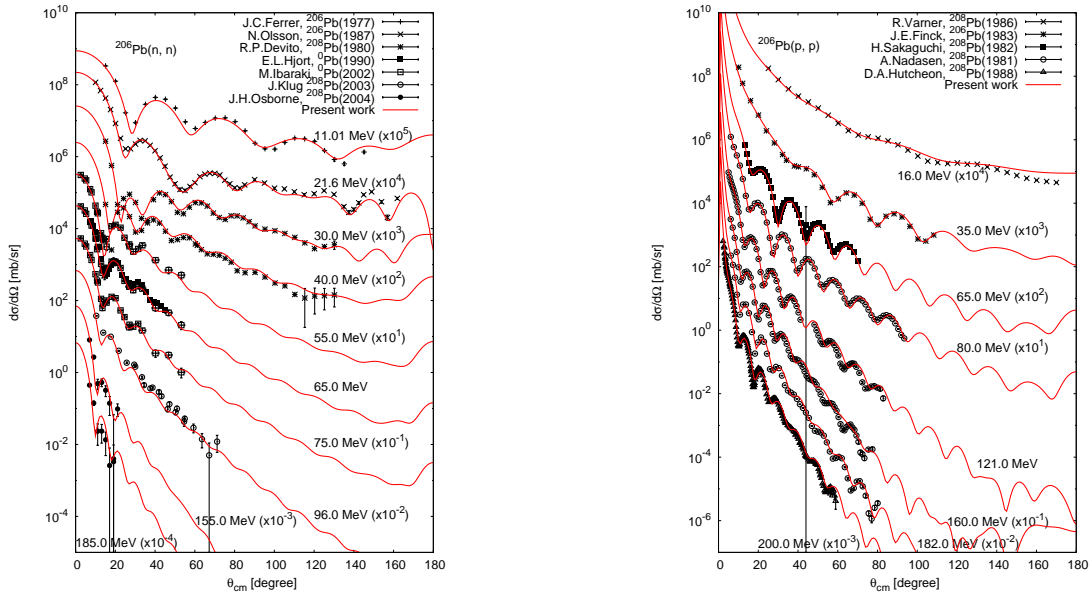


Fig. 2: Present evaluations and measured data<sup>9)</sup> for neutron- and proton-induced angular-differential elastic-scattering cross sections on  $^{206}\text{Pb}$ .

### 3 The GNASH calculations

The GNASH code was utilized for calculating energy-differential cross sections for the productions of light-particles (neutron, proton, deuteron, triton,  $^3\text{He}$  and  $\alpha$ -particle) and isotope-production cross sections. The code was basically the same one employed in the LA150 evaluations. In the Monte Carlo simulations for high energy applications, the angular distributions of emission particles are important. Therefore, double-differential cross sections were also calculated for the emitted particles by using the Kalbach angular-distribution systematics.<sup>8)</sup>

The exciton model has some adjustable parameters such as the single-particle state

density parameter  $g$  and the average squared matrix element  $|M|^2$ . The evaluation of double-differential cross sections was implemented by adjusting these parameters. The results deduced in the laboratory frame are compared with available experimental data and the LA150 evaluations in **Fig. 3** for  $(n, xp)$  and **Fig. 4** for  $(p, xn)$  and  $(p, xp)$ . The evaluations of isotope-production cross sections are presented together with experimental data and the LA150 evaluations in **Figs. 5** and **6**. These results show that the evaluated cross sections give good agreements with experimental data. However, there was large discrepancy between evaluated and experimental isotope-production cross sections for some residual nuclei. One of the reasons might be due to some imperfect descriptions of the level density parameters.

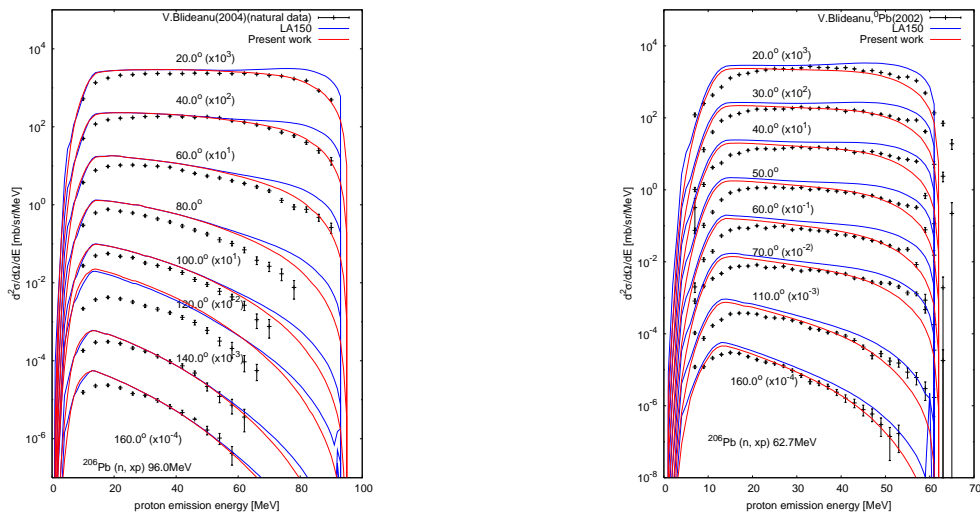


Fig. 3: Present evaluations and experimental data<sup>9)</sup> of double-differential cross sections for  $(n, xp)$  reactions on  $^{206}\text{Pb}$  at 96 MeV, and 62.7 MeV.

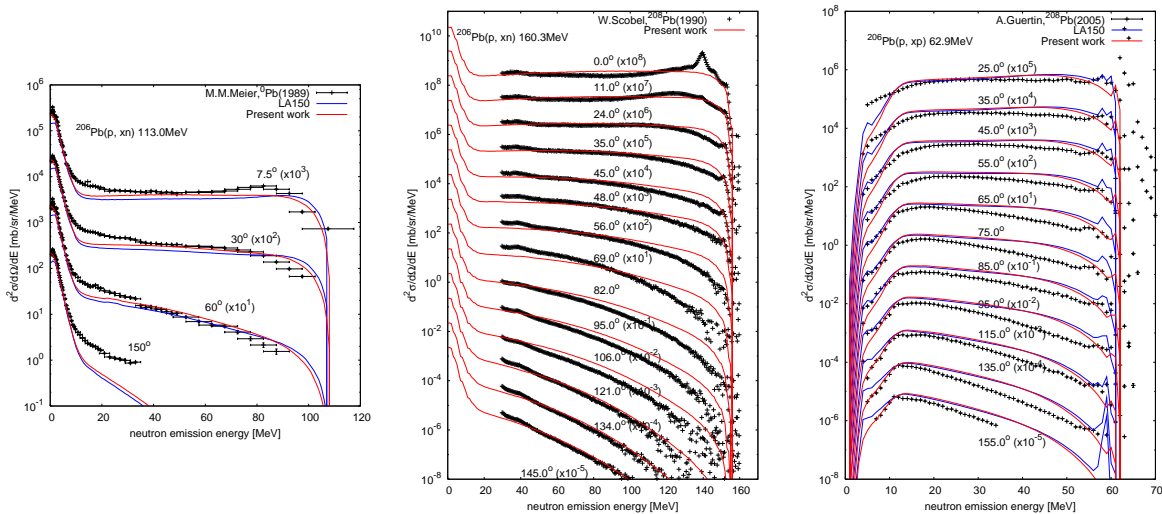


Fig. 4: Present evaluations and experimental data<sup>9)</sup> of double-differential cross sections for  $(p, xn)$  and  $(p, xp)$  reactions on  $^{206}\text{Pb}$  at 113 MeV, 160.3 MeV, and 62.9 MeV.

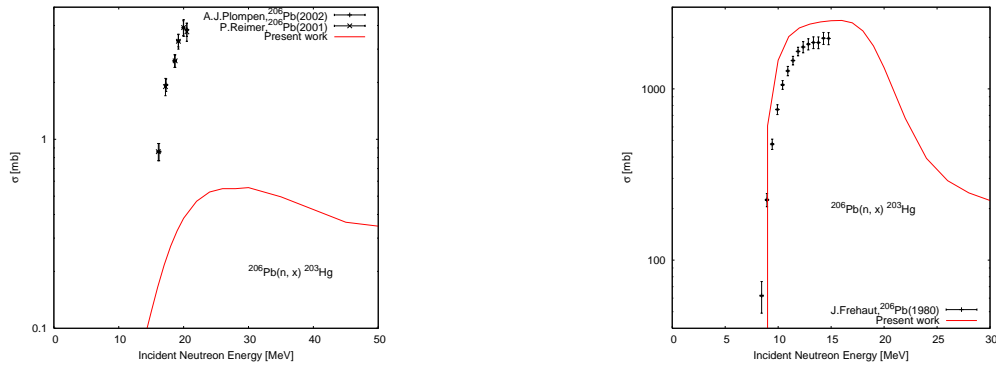


Fig. 5: Present evaluations, experimental data<sup>9)</sup> of isotope-production cross sections for neutron incidence.

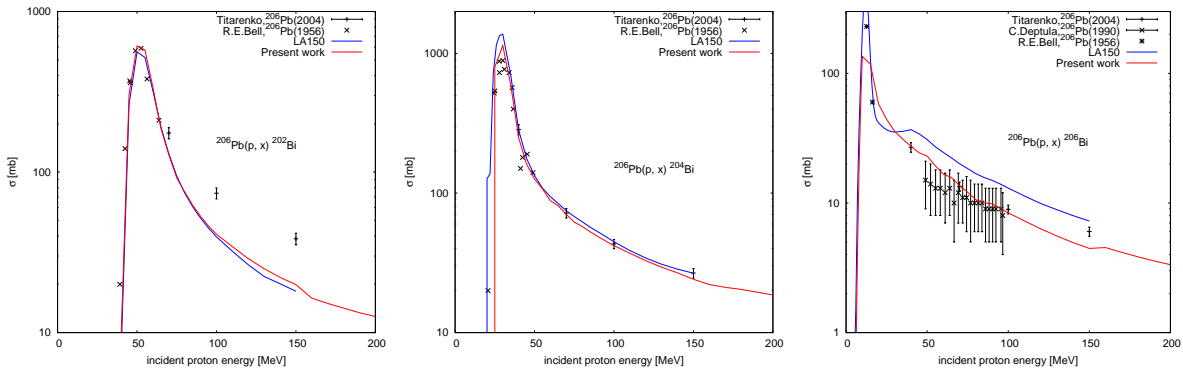


Fig. 6: Present evaluations, experimental data<sup>9)</sup> and LA150 evaluations of isotope-production cross sections for proton incidence.

## 4 Summary

The evaluation of cross sections for  $^{206}\text{Pb}$  was performed for neutron- and proton-induced reactions by using the ECIS-96 and the GNASH code. The energy range of evaluation was from 20 to 200 MeV. The global optical potentials were adopted to allow the continuous evaluation for the incident energy. The optical model potential parameters were determined to give good agreements with experimental data of total and angular-differential elastic scattering cross sections. The GNASH code was used for evaluations of energy-differential particle-production cross sections and isotope-production cross sections. Double-differential cross-sections of the emitted particles were calculated on the basis of the Kalbach systematics. Present evaluations were compared with the available experimental data and LA150. Good overall agreements were obtained. However, there was large discrepancy between evaluated and experimental isotope-production cross sections for some residual nuclei.

## Acknowledgments

The authors would like to appreciate technical supports for all the members of Nuclear Data Center at Japan Atomic Energy Agency.

## References

- 1) T. Fukahori, Y. Watanabe, N. Yoshizawa, F. Maekawa, S. Meigo, C. Konno, N. Yamano, AY Konobeyev, and S. Chiba, *J. Nucl. Sci. Technol. Suppl.*, **2**, 25, (2002).
- 2) J. Raynal, Notes on ECIS94, Report CEA-N-2772, Centre d'Etude de Saclay CEA, Saclay, France (1994).
- 3) P. G. Young, E. D. Arthur, M. B. Chadwick, in: Workshop on Nuclear Reaction Data and Nuclear Reactors, Trieste, Italy, 15 April-17 May 1996, p. 227.
- 4) M. B. Chadwick, P. G. Young, S. Chiba, S. C. Frankle, G. M. Hale, H. G. Hughes, A. J. Koning, R. C. Little, R. E. MacFarlane, R. E. Prael, *et al.*, *Nucl. Sci. Eng.*, **131**, 293 (1999).
- 5) E. Sh. Soukhovitskii, S. Chiba, O Iwamoto, *et al.*, JAERI-Data/Code 2005-002 (2005).
- 6) A. J. Koning, J. P. Delaroche, *Nucl. Phys.*, **A713**, 231 (2003).
- 7) S. Kunieda, S. Chiba, K. Shibata, A. Ichihara, Efrem Sh. Sukhovitskii, published to *J. Nucl. Sci. Technol.*, **44**.
- 8) C. Kalbach, *Phys. Rev. C*, **37**, 2350 (1988).
- 9) EXFOR cross section data online at <http://www.nea.fr/html/dbdata/x4/welcome.htm>